CONTINUOUS RESISTANCE HEATING TECHNOLOGY FOR HIGH-SPEED CARBON FIBRE PLACEMENT PROCESSES

Yannis Grohmann
German Aerospace Center (DLR)
Institute of Composite Structures and Adaptive Systems
Ottenbecker Damm 12
21684 Stade, Germany

ABSTRACT

The Continuous Resistance Heating Technology (CoRe HeaT) is an alternative to state-of-the-art heating systems for carbon fibre placement processes. It allows rapid heating with minimal reaction times and thus offers the potential to increase productivity for suitable processes. A brief overview of the technology is given with a focus on the development of a temperature prediction model. First experiments show how to validate the model for new materials. The aim is to achieve optimized heat generation by implementing the model into the temperature controller.

1. INTRODUCTION

Basic principle of the CoRe Heating Technology is to use the Joule effect to directly heat the carbon fibres intrinsically via their own resistance. Compared to today's technology, this enables higher heating rates and offers lower response times, which can be used to increase the productivity for a variety of manufacturing processes.
A prototype end effector equipped with a CoRe Heating unit that is used for Automated Fibre Placement (AFP) and winding has been built at the Center for Lightweight-Production-Technology (ZLP®) of the German Aerospace Center in Stade, Germany. With manufacturing trials and automated test laminate production, the influence of the technology on preforms and final parts is determined. Test specimens are produced once with CoRe HeaT and once with an infrared heater to compare the results. In order to improve the temperature control of the new heating technology, a thermal model is developed, experimentally investigated and discussed.

2. THEORETICAL MODEL

A precise temperature control during production processes using carbon fibre materials is essential to ensure a consistently high quality, especially for parts produced with thermoplastic prepreg materials [1, 2]. A thorough understanding of the process is needed. Regarding AFP and winding, many temperature models have been published. The review of Tilman Orth [3] gives a good overview of current approaches as well as their differences and similarities. Foundation for all thermal models is the first law of thermodynamics, which is the principle of conservation of energy. Regarding the energy balance, the base for a thermal model can be expressed as

$$Q_{in} - Q_{out} + E_{gen} = \Delta E_{ths} \qquad 1$$

where the sum of all heat transfer processes ($Q_{in} - Q_{out}$) and the amount of thermal energy generated (E_{gen}) are equal to the total change of thermal energy of the system (ΔE_{ths}) [4].
A short overview on the basic heat transfer mechanisms is given in Sections 2.1, 2.2 and 2.3. One of the main differences to other heating technologies is the thermal energy generated

volumetrically within the fibres, which is described in Section 2.4. The formula to calculate temperature changes using the energy balance is described in Section 2.5.
The first step in developing the model is to define the system boundaries. With the aim of predicting the maximum occurring process temperature of the carbon fibre material, the center of the theoretical model is a tow segment moving through space and time, which is known as the Lagrangian approach. The temperature gradients in thickness direction and across the width of that segment are assumed to be zero due to the use of thin materials and a volumetric heating process. Reducing the length of the segment to an infinitesimal small element, the temperature gradient in length direction is also neglected. The goal is to determine the temperature gradient dT/dt of that element in [K/s] with T as the material's temperature and t as the time.
Figure 1 shows the consolidation roller of an AFP end effector and a tow that is getting heated during layup with a placement speed v in [m/s]. First sector of the model is the tow in front of the consolidation roller. The input temperature T1 is measured with a thermal imaging sensor like a pyrometer or thermographic camera. Heat losses in sector 1 are defined by convection and radiation on both sides of the tow (see Section 3.2.1). End of the first sector and beginning of the second sector with a material temperature of T2 is the point where the tow gets into contact with the consolidation roller. In that sector additional conductive cooling on the consolidation roller side of the carbon fibre material has to be considered (see Section 3.2.2). At the end of sector 2, the tow gets into contact with the laminate and the inserted energy quickly dissipates into the laminate. With the additional cooling from the laminate and reduced heat generation, it can be assumed that the maximum process temperature is reached at that point, provided that an appropriate heating strategy and suitable process parameters were chosen. The scope of this paper therefore ends at the beginning of sector 3 with the maximum temperature T3. Further cooling processes in sector 3 and 4 will not be considered.

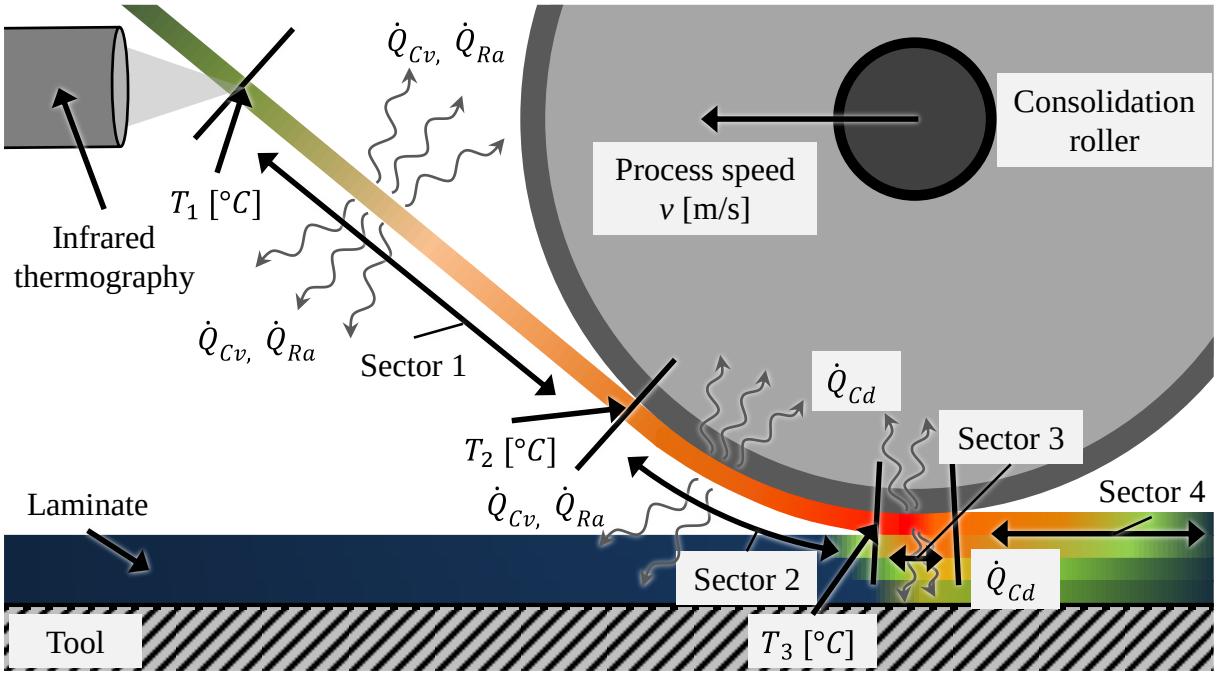

Figure 1: The AFP process and the different temperature zones for the model

2.1 Conductive heat transfer

Conduction is the transfer of energy between two adjacent particles. However, the heat transfer between a carbon fibre tow and a consolidation roller normally is a mixture of conductive, convective and radiative heat transfers, due to undefined surface contacts and air pockets in between. Nevertheless, since the conductive heat transfer mechanisms are the most dominant, in this paper it will still be referred to as conductive heat transfer. Using Newton's law of cooling is common to express the heat transfer between the tow and the roller:

$$\dot{Q}_{Cd} = h_{Cd} \cdot A_{Cd} \cdot (T_{S1} - T_{S2}) \quad (2)$$

Where h_{Cd} is the conductive heat transfer coefficient in [W/m²K], A_{Cd} is the contact surface area in [m²] and T_{S1} and T_{S2} the temperatures of the surfaces in contact in [K]. [4]
The heat transfer coefficient can only be determined by experiments. Even though some values can be found in literature, several parameters have a big impact on the conductive heat transfer. If not taken into account, the heat transfer coefficient can vary significantly, even for the same material combinations. For example, Grouve found several values for the heat transfer coefficient of carbon thermoplastic composites in contact with a steel tooling, ranging from 400 to 1000 W/m²K [5]. Therefore experiments were carried out to get more accurate results (Section 3.2.2).

2.2 Convective heat transfer

Convection is the energy transfer between a solid surface and an adjacent fluid in motion. To describe the phenomenon, Newton's law of cooling is commonly used.

$$\dot{Q}_{Cv} = h_{Cv} \cdot A_{Cv} \cdot (T_S - T_\infty) \quad (3)$$

Here h_{Cv} is the convection heat transfer coefficient in [W/m²K], A_{Cv} is the surface area taking part in the convective heat transfer in [m²], T_S is the surface temperature and T_∞ is the temperature of the fluid of the surrounding area in [K]. [4]
The convection heat transfer coefficient is also determined experimentally and is mainly influenced by the surface geometry, the properties of the surrounding fluid and the temperatures. Stokes-Griffin uses values ranging from 5 W/m²°C for a surface temperature of 20 °C to 17.1 W/m²°C for a 300 °C surface [6]. However, a constant value at the average temperature is often used, since it is sufficiently accurate. Unfortunately, detailed information regarding the temperature ranges are usually missing. Furthermore, these values should only be used at process speeds well below 500 mm/s when free convection can be assumed. Studies on forced convection cooling show that the heat transfer coefficient can increase significantly with increasing wind speed [7]. Although experiments to determine the convective heat losses have been carried out (Section 3.2.1), forced convection cooling has not yet been validated.

2.3 Radiative heat transfer

Radiation is the energy emitted in forms of electromagnetic waves. If a body has a higher temperature than the surrounding surfaces, heat energy is lost in the form of thermal radiation. The radiation emitted by a surface can be expressed by

$$\dot{Q}_{Ra} = \varepsilon \cdot \sigma \cdot A_S \cdot (T_S^4 - T_\infty^4) \quad (4)$$

where ε is the emissivity of the surface, σ the Stefan–Boltzmann constant with a value of $5.67 \cdot 10^{-8} \frac{W}{m^2 K^4}$, A_S the surface area in [m²], T_S the temperature of the surface and T_∞ the temperature of the surroundings in [K]. [4]

Some models neglect the influence of radiative heat losses. In Section 3.2, experimental validations show the influence of radiative heat losses in comparison to convective and conductive heat losses.

2.4 Heat generation – ohmic heating/ Joule heating

Heat can be generated within carbon fibre tows by conversion of mechanical, chemical or in this case electrical energy into thermal energy. The relationship between the thermal energy that is generated and the electrical energy needed for that is described by Joule's first law, also known as the Joule effect or ohmic/resistance heating:

$$E_{El} = I^2 \cdot R \cdot t \qquad 5$$

Where I is the current running through the fibres in [A], R being the resistance in [Ω], t the time in [s] and E_{El} the thermal energy generated in [J]. [8]
The carbon fibre tow is modeled as a homogenous ohmic resistor. The model concentrates on an infinitesimal element. All elements lined up after each other build a series of resistors. In an electrical circuit with ohmic resistors in series, the electrical current is the same at every point of the circuit. Therefore, using the resistance of an element and the current running through it, the thermal energy generated within that element gets calculated.

2.5 Thermal energy balance of system

A general thermal energy balance for a closed system is

$$\Delta E = m \cdot c \cdot \Delta T \qquad 6$$

where m is the systems mass in [kg], c the specific heat capacity of the systems material in [J/kgK] and ΔT the change of the systems temperature in [K] [4]. Using that formula, the temperature of the system can be predicted at any time. With the time derivative, the heating rate $\frac{\mathrm{d}T}{dt}$ in [K/s] can be estimated.
With formulas 1-7, all basic physical equations and relationships have been worked out and the temperature prediction model for using the CoRe Heating Technology can be calculated. In order to do so, all material related parameters and coefficients have to be determined, which is done in the next chapter.

3. EXPERIMENTAL VALIDATION

To validate the theoretical model, several experiments were set up. The dry fibre AFP material used for validation has just been developed in recent years. Therefore all material related properties that are needed for calculations have been determined experimentally (Section 3.1). Static validation trials using the CoRe Heating Technology were carried out to determine all relevant heat transfer coefficients (Section 3.2).

3.1 Material properties

Dry fibre AFP tows come in different widths and aerial weights. A common configuration for AFP processes is a ¼" or 6.35 mm wide tape with an aerial weight around 200 g/m². The material is enhanced with a thermoplastic binder with a melting point around 160 °C. The properties relevant for temperature modeling are discussed in detail in the following sections.

3.1.1 Linear mass density

The linear mass density of a carbon fibre tow, is the amount of mass per unit length. While the SI unit would be kilograms per meter, for textiles it is more common to use the unit tex, which is equivalent to grams per kilometer. This material property was simply determined by cutting material stripes with a length of 100 mm and measuring their weight with a precision balance. The test material samples had an average of 1400 tex.

3.1.2 Resistivity

The resistance of the material is needed in order to calculate the amount of thermal energy that is generated according to formula 5. For the infinitesimal element, the length specific resistance has to be determined. This was done with an ohmmeter by measuring several specimens with different tow lengths, ranging from 100 mm to 2500 mm. For each length, three samples were tested. With a linear interpolation of the results, a formula for the length specific resistance R_l in [Ω/m] is determined. Figure 2 (left side) shows the result for the test material.
As carbon fibres have a negative temperature coefficient, their resistivity decreases with rising temperatures. With the aim of precise temperature modeling, the change of resistivity while heating up needs to be taken into account. For this purpose, 2500 mm long specimens were slowly heated to 250 °C in an oven, while their resistance was measured regularly. Different carbon fibre materials were tested and all were showing a linear proportional relationship between temperature and resistance. Figure 2 (right side) is showing the measurement results for the temperature dependent length specific resistance of the dry fibre AFP test material.

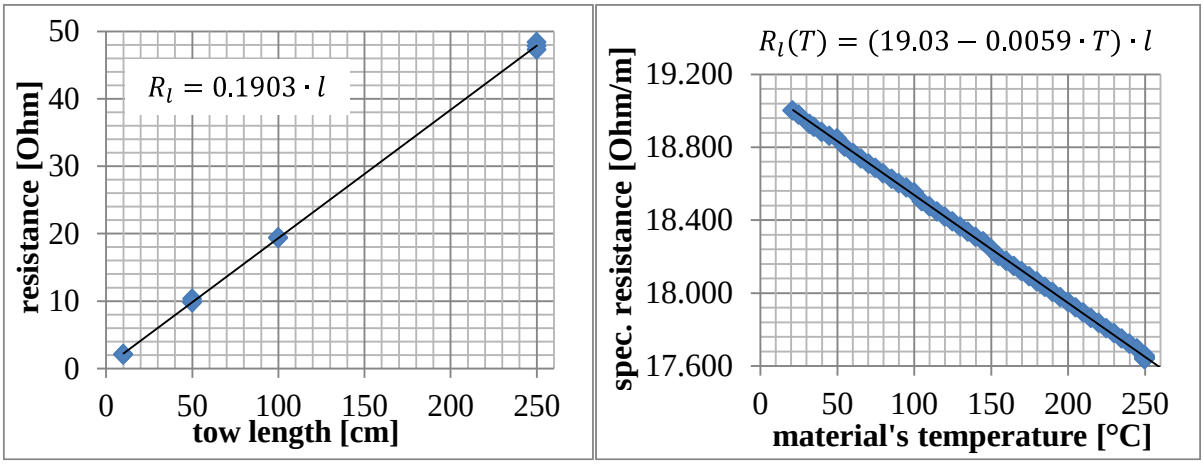

Figure 2: Results of resistivity measurements

3.1.3 Heat capacity

The heat capacity is the physical property of a material that defines the amount of heat energy needed to change the temperature of a given mass of that material. Commonly used is the specific heat capacity in [J/kgK]. The result shown in Figure 3 was obtained by temperature modulated differential scanning calorimetry (TMDSC). To get the length specific heat capacity c_l in [J/mK], the results are multiplied with the linear mass density T_t in [g/km], which was obtained in Section 3.1.1.

$$c_l = c \cdot T_t \qquad 7$$

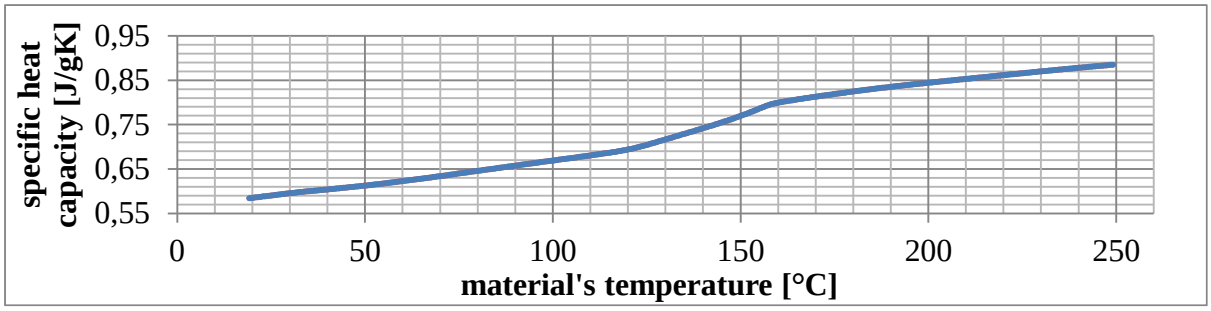

Figure 3: Specific heat capacity over temperature

3.1.4 Emissivity

The emissivity of the material's surface has an influence on the radiative heat transfer according to Formula 4. Additionally, it affects the accuracy of the experimental results, since a thermal imaging camera is used to measure the temperature and the emissivity has an impact on the results of such a camera. The emissivity of the test material was therefore determined experimentally based on the ASTM E1933 standard. According to that, the material's temperature is logged with a thermocouple while getting heated and the results are compared with the data from the thermal camera. An emissivity of 0.85 gave good results and matched a value found in literature [9].

3.2 Validation trials

First validation trials are conducted to determine how much heating power is lost due to heat transfer processes. The tow gets heated with a constant predefined power in a closed test environment. A thermal camera is used for temperature logging. When the material has reached the power-specific maximum temperature and it doesn't change anymore, the thermal system is balanced. At that point, the heating energy generated by resistance heating is equal to the energy lost due to all heat transfer processes. These can now easily be determined by following the steps explained in the next sections.

3.2.1 Free convection and radiative energy losses

In Sector 1, thermal energy is lost due to convective and radiative heat transfer processes on both sides of the carbon fibre tow (see Figure 4). As explained in Section 3.2, the material gets heated with different current settings until a temperature balance is reached. Using a constant current source and the temperature dependent length specific resistance from Section 3.1.2, results in the length specific heating power in [W/m]. Current settings starting at 0.7 A up to 1.9 A led to material temperatures ranging from 58 °C to 185 °C.

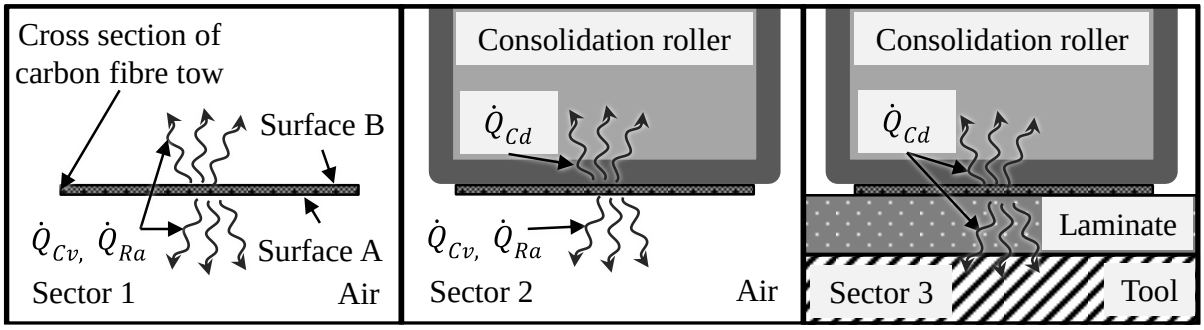

Figure 4: Overview of the heat transfer processes within the different model sectors

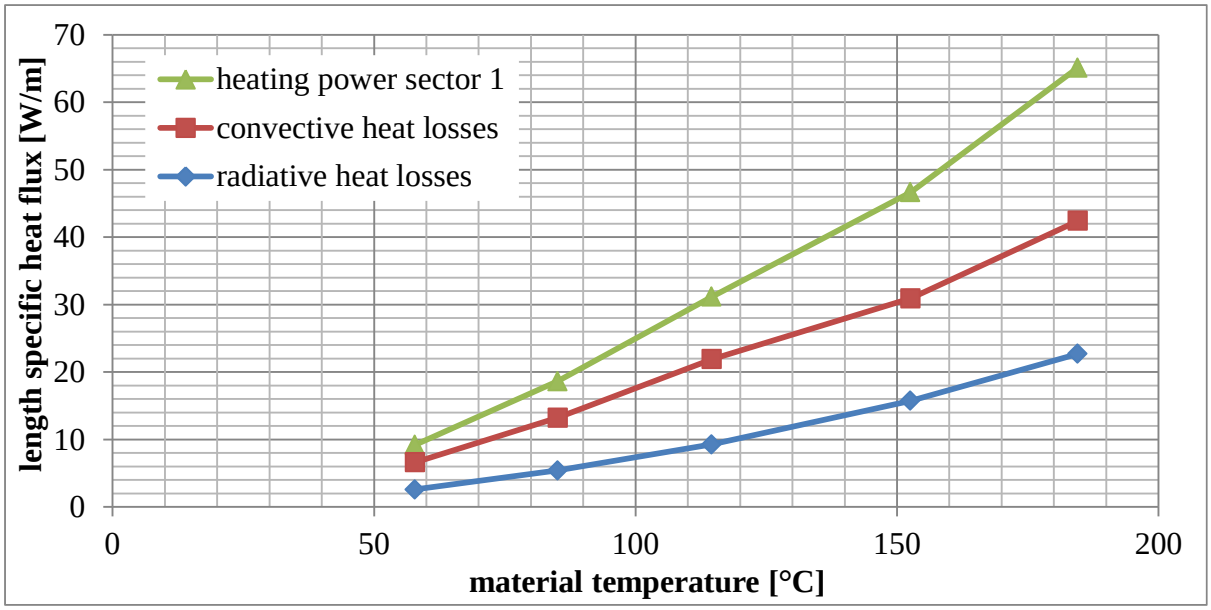

Figure 5: Heating power lost due to convective and radiative heat transfer processes

By measuring the material's temperature and the surrounding temperature, the radiative heat losses can be calculated according to Formula 4. If the circumference of the material is used instead of a full surface, the equation gives the length specific radiative heat losses in [W/m]. The length specific convective heat losses $\dot{Q}_{Cv\_l}$ can then be calculated by subtracting the length specific radiative heat losses $\dot{Q}_{Ra\_l}$ from the length specific heating power $\dot{E}_{El\_l}$.

$$\dot{Q}_{Cv\_l} = \dot{E}_{El\_l} - \dot{Q}_{Ra\_l} \qquad 8$$

The results are shown in Figure 5.

3.2.2 Convective, radiative and conductive energy losses

Entering sector 2, surface B of the carbon fibre material gets into contact with the consolidation roller (see Figure 4). Conductive heat transfer mechanisms start to dominate the thermal energy losses. Surface A of the material is still exposed to convective and radiative heat transfers only. For the test setup, a silicone rubber roller and an aluminum roller were tested. Using the aluminum roller, a temperature balance was reached in less than 1.5 seconds. The silicone rubber roller tests however were stopped before a temperature balance was reached. After about 2 seconds, a slow but constant increase of the temperature could be observed. This can be explained with an increasing surface temperature of the roller, which reduces the cooling effect. The final results of the silicone roller are therefore an estimation where the balanced temperature was approximated.

Using the same procedure and the results from Section 3.2.1, the length specific conductive heat losses in [W/m] for surface B can be determined. With the simplification that surface A and B are equal in size, the energy lost on surface A can be expressed as half of the total amount of power lost in sector 1. This leads to

$$\dot{Q}_{Cd\_l} = \dot{E}_{El\_l} - 0.5 \cdot \dot{Q}_{S1\_l} \qquad 9$$

with $\dot{Q}_{Cd\_l}$ as the length specific heat transfer losses due to the conductive contact to the consolidation roller and $\dot{Q}_{S1\_l}$ as the total heat transfer losses from sector 1 that were already determined in the previous section. The results are shown in Figure 6.

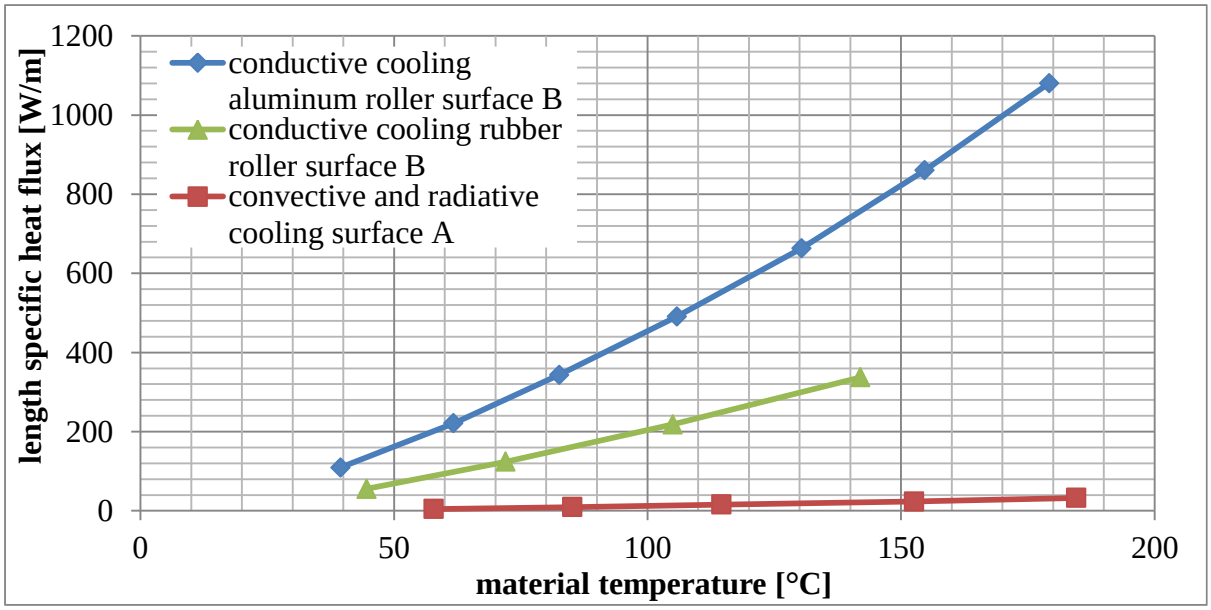

Figure 6: Conductive heating losses compared to convective and radiative heating losses

Regarding sector 3, surface A gets into contact with the laminate while surface B is still in contact with the consolidation roller. Due to the compression force of the roller, which leads to an increased contact surface between roller and tow, it is assumed that the conductive cooling effect of the consolidation roller is increasing. However, the additional conductive cooling effect from the contact to the laminate has a much bigger impact. As explained in Chapter 2, it is assumed that the cooling effects will outweigh the heat generation in sector 3 and the scope of this paper's model ends. Therefore the cooling effect of the laminate has not yet been investigated.

3.2.3 Thermal Energy balance – temperature prediction

With the results from 3.2.1 and 3.2.2 as well as the results from Section 3.1, it is possible to calculate the heating rate dT/dt using the previously discussed formulas. For a tow that gets heated in sector 1, the combination of all collected results leads to the following formula

$$\frac{I^2 \cdot R_l(\mathrm{T}) - c_{tow} \cdot [h_{Cv}(\mathrm{T}) \cdot (T(t) - T_\infty) + \varepsilon \cdot \sigma \cdot (T(t)^4 - T_\infty^4)]}{c_l(\mathrm{T})} = \frac{\mathrm{d}T}{dt} \qquad 10$$

with c_{tow} as the circumference of the tow. For sector 2 the term for dT/dt changes to

$$\frac{I^2 \cdot R_l(\mathrm{T}) - 0.5 \cdot c_{tow} \cdot [h_{Cv}(\mathrm{T}) \cdot (T(t) - T_\infty) + h_{Cd}(\mathrm{T}) \cdot (T(t) - T_S) + \varepsilon \cdot \sigma \cdot (T(t)^4 - T_\infty^4)]}{c_l(\mathrm{T})} \qquad 11$$

Plots of the temperature development of a tow segment were calculated using the model and compared to the real test data from the experiments from Section 3.2.1. The model's predictions were approximately 30% higher than the measured temperatures. Reducing the model's results by this amount led to a curve that almost perfectly matched the actual results. A comparison of a modeled curve, where the temperature results were reduced by 30%, to a curve of one of the tests of Section 3.2.1, is shown in Figure 7.

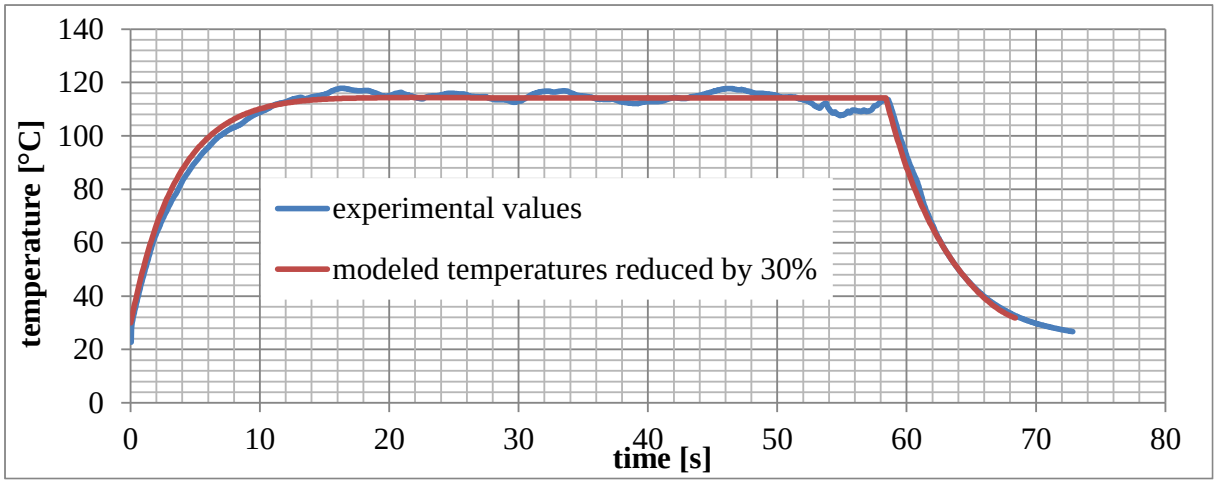

Figure 7: Plot of experimental results in comparison to tweaked modeled results

For the simulation of the tow temperature during layup and determination of the maximum occurring temperature T3, the input temperature T1, the rollers surface temperature T_S, the temperature of the surroundings T_∞, the placement speed v and the length of sector 1 and 2 as well as the current I within the tow are needed. However, for a dynamic process with speeds > 0.5 m/s, the change from free convection to forced convection cooling could have an important impact which has not yet been determined. Also the current results with a 30% offset are not satisfying. Therefore validation experiments for a dynamic process were postponed.

3.3 Discussion

In the previous chapter it was shown, that the model's results are approximately 30% higher than real measured values. After evaluating all possible influences, the current assumption is that the specific heat capacity value is too low by exactly this value. A review of the test method was made and one of the problems identified is the soft and uneven surface property of the dry fibre material. The dry fibre tapes are an undefined mixture of carbon fibres, air and additional binder. For optimal results using the DSC test method, a perfect contact from the material samples to the heated surface of the DSCs crucible is needed and additional air pockets within the material should ideally be eliminated. A possible solution to fix this problem could be the preparation of fully cured samples including the matrix system. According to literature, it is possible to calculate the specific heat of carbon fibres embedded inside a matrix system by rule of mixture [10].

4. MANUFACTURING TRIALS

Manufacturing trials were carried out to investigate the influences of the heating technology on preforms as well as final parts. A prototype AFP end effector that can be equipped with an infrared heater or the CoRe Heating Technology was used for automated test laminate production. During the production of interlaminar shear strength (ILSS) test specimen, a difference between the influence of infrared and CoRe HeaT on bulking and permeability of the preforms was found. However, after resin infusion, a comparison of the mechanical properties of the final parts produced with infrared or CoRe HeaT showed no differences. [11]

5. CONCLUSIONS AND OUTLOOK

In Chapter 2, the theoretical basics for a temperature prediction model for CoRe HeaT were developed. With the experiments from Chapter 3, first validations of the model were possible. The results are promising and can already be used to improve the temperature control of the technology. A final validation during layup with high speeds is planned after the determination of forced convection coefficients and solving the issue with the specific heat capacity.
Furthermore, trials with different material widths, areal weights and different material types are planned for thorough validation. Additional manufacturing trials will be carried out to further understand and validate any possible influences on part production. With a new winding test setup, future manufacturing trials of tubes and rings with windings speeds exceeding 2 m/s will be possible.

6. REFERENCES

[1] A. Kollmannsberger, "Heating characteristics of fixed focus laser assisted Thermoplastic-Automated Fiber Placement of 2D and 3D parts," 2019.

[2] M. Schäkel, H. Janssen and C. Brecher, "Model-predictive Control for the Automated Production of Thermoplastic Composite Pressure Vessels," in *ITHEC, Bremen, Germany*, 2018.

[3] T. Orth, C. Weimer, M. Krahl and N. Modler, "A review of radiative heating in automated layup and its modelling," *Journal of Plastics Technology*, vol. 13, p. 91–125, 2017.

[4] Y. A. Cengel, Heat Transfer: A Practical Approach. 2nd Edition, McGraw-Hill Professional, New York, USA, 2002.

[5] W. Grouve, "Weld strength of laser-assisted tape-placed thermoplastic composites," 2012.

[6] C. M. Stokes-Griffin, "A combined Optical-Thermal Model for Laser-Assisted Fibre Placement of Thermoplastic Composite Materials," 2015.

[7] M. Janicki, J. Banaszczyk, G. De Mey, M. Kaminski, B. Vermeersch and A. Napieralski, "Application of structure functions for the investigation of forced air cooling," in *13th International Workshop on Thermal Investigation of ICs and Systems (THERMINIC)*, 2007.

[8] W. Zeller and A. Franke, Das physikalische Rüstzeug des Ingenieurs. 11. verbesserte Auflage, Technik-Tabellen-Verlag Fikentscher & Co, Darmstadt, Germany, 1977.

[9] M. Di Francesco, L. Veldenz, G. DellAnno and K. Potter, "Heater power control for multi-material, variable speed Automated Fibre Placement," *Composites Part A: Applied Science and Manufacturing*, vol. 101, p. 408–421, 10 2017.

[10] H. Schürmann, Konstruieren mit Faser-Kunststoff-Verbunden. 2nd Edition, Springer Berlin Heidelberg, 2007.

[11] Y. Grohmann, "A new heating method for faster fibre placement," in *11th International Conference on Manufacturing of Advanced Composites, Nottingham, UK*, 2018.